

Lamin-B1 contributes to the proper timing of epicardial cell migration and function during embryonic heart development

Joseph R. Tran, Xiaobin Zheng, and Yixian Zheng*

Department of Embryology, Carnegie Institution for Science, Baltimore, MD 21218

ABSTRACT Lamin proteins form a meshwork beneath the nuclear envelope and contribute to many different cellular processes. Mutations in lamins cause defective organogenesis in mouse models and human diseases that affect adipose tissue, brain, skeletal muscle, and the heart. In vitro cell culture studies have shown that lamins help maintain nuclear shape and facilitate cell migration. However, whether these defects contribute to improper tissue building in vivo requires further clarification. By studying the heart epicardium during embryogenesis, we show that Lb1-null epicardial cells exhibit in vivo and in vitro migratory delay. Transcriptome analyses of these cells suggest that Lb1 influences the expression of cell adhesion genes, which could affect cell migration during epicardium development. These epicardial defects are consistent with incomplete development of both vascular smooth muscle and compact myocardium at later developmental stages in Lb1-null embryos. Further, we found that Lb1-null epicardial cells have a delayed nuclear morphology change in vivo, suggesting that Lb1 facilitates morphological changes associated with migration. These findings suggest that Lb1 contributes to nuclear shape maintenance and migration of epicardial cells and highlights the use of these cells for in vitro and in vivo study of these classic cell biological phenomena.

Monitoring Editor

Tom Misteli
National Cancer Institute, NIH

Received: Jun 24, 2016

Revised: Oct 11, 2016

Accepted: Oct 12, 2016

INTRODUCTION

Lamins are type V intermediate-filament proteins found in the nucleus of metazoan cells (Dechat *et al.*, 2010; Burke and Stewart, 2013; Gruenbaum and Foisner, 2015). The lamins are structurally conserved, and many animals have two classes of lamin, A and B type, which arise from separate genes. In humans, *LMNA* encodes for all A-type lamins, whereas two separate genes, *LMNB1* and *LMNB2*, encode for B-type lamins. A number of human diseases are caused by mutations in these genes. For example, mutations in *LMNA* can cause dilated cardiomyopathy, Emery–Dreifuss muscular dystrophy, and Hutchinson–Gilford progeria, among others (Bonne *et al.*, 1999; Fatkin *et al.*, 1999; De Sandre-Giovannoli *et al.*, 2003; Eriksson *et al.*, 2003). Of interest, many of these diseases are tissue

restricted, with adipose tissue, brain, heart, and skeletal muscle being more sensitive to perturbations in lamin proteins. The basis for this remains unclear.

Recent studies of B-type lamin highlight the importance of these proteins in organogenesis of the developing mouse embryo. Unlike lamin-A, lamin-B1 (Lb1) is essential for postnatal life, and developing *Lmn1* (*Lb1*)-null embryos show defective organogenesis of the brain, diaphragm, and lung (Sullivan *et al.*, 1999; Coffinier *et al.*, 2011; Kim *et al.*, 2011). An insertional mutant that produces only the N-terminal half of Lb1 also revealed a role in bone development (Vergnes *et al.*, 2004). The developmental defect in the brain, which was best characterized, appeared as a disorganization of brain cortical layers and was attributed to defective interkinetic nuclear migration, neuronal cell migration, and spindle orientation in neural progenitor cells (Coffinier *et al.*, 2011; Kim *et al.*, 2011).

Although lamins appear to be nonessential for cell viability, many processes, including transcriptional/chromatin regulation, mitotic spindle morphology or orientation, signal transduction, cell morphology/migration, and others, are affected by defects in these proteins (Imai *et al.*, 1997; Tsai *et al.*, 2006; Muchir *et al.*, 2007; Guelen *et al.*, 2008; Scaffidi and Misteli, 2008; Hernandez *et al.*, 2010; Coffinier *et al.*, 2011; Kim *et al.*, 2011, 2013; Chen *et al.*, 2013; Guo *et al.*, 2014; Guo and Zheng, 2015; Zheng *et al.*, 2015). Further,

This article was published online ahead of print in MBoC in Press (<http://www.molbiolcell.org/cgi/doi/10.1091/mbc.E16-06-0462>) on October 19, 2016.

*Address correspondence to: Yixian Zheng (zheng@ciwemb.edu).

Abbreviations used: Lb1, lamin-b1; *Lb1*, *Lmn1*; Wt1, Wilm's tumor 1.

© 2016 Tran *et al.* This article is distributed by The American Society for Cell Biology under license from the author(s). Two months after publication it is available to the public under an Attribution–Noncommercial–Share Alike 3.0 Unported Creative Commons License (<http://creativecommons.org/licenses/by-nc-sa/3.0>).

“ASCB®,” “The American Society for Cell Biology®,” and “Molecular Biology of the Cell®” are registered trademarks of The American Society for Cell Biology.

B-type lamin level is regulated in processes such as aging and cell stress and upon senescence, which can contribute to certain cellular responses, such as inflammation (Shimi *et al.*, 2011; Freund *et al.*, 2012; Chen *et al.*, 2015; Tran *et al.*, 2016). How lamins function in these various contexts is not well understood, but it is generally accepted that lamins influence nuclear shape and the migratory behavior of cells (Dahl *et al.*, 2008). Alteration in nuclear shape, often seen as a structural blebbing, is perhaps the most common *in vitro* phenotype in lamin mutants and has been documented *in vivo* (Sullivan *et al.*, 1999; Liu *et al.*, 2000; Guillemain *et al.*, 2001; Goldman *et al.*, 2004; Vergnes *et al.*, 2004; Lammerding *et al.*, 2006; Jung *et al.*, 2013). However, nuclear deformation also occurs as part of normal cell biology during cell migration and is modulated by nuclear stiffness and lamin-A levels (Lammermann *et al.*, 2008; Shin *et al.*, 2013; Wolf *et al.*, 2013; Davidson *et al.*, 2014; Ribeiro *et al.*, 2014; Lautscham *et al.*, 2015). Accordingly, defective migration is seen in different lamin mutant cell lines *in vitro* and in *Lb1*-null neuronal populations *in vivo* (Lee *et al.*, 2007; Coffinier *et al.*, 2011; Kim *et al.*, 2011, 2014; Pacheco *et al.*, 2014; Chang *et al.*, 2015a), but it remains unclear how nuclear shape changes are correlated with cell migratory behavior *in vivo*.

During heart development, cells migrate from an extracardiac outgrowth called the proepicardial organ at approximately embryonic day 9.0 (E9.0) and populate the surface of the heart by E11.0 (Olivey and Svensson, 2010; von Gise and Pu, 2012). These cells, called epicardial cells, form a continuous epithelial sheet (epicardium) surrounding the myocardium and have been identified by their expression of Wilm's tumor 1 (*Wt1*), T-box 18 (*Tbx18*), *Tcf21*, *Scleraxis* (*Scx*), or *Semaphorin3D* (*Sema3D*; Moore *et al.*, 1998; Cai *et al.*, 2008; Katz *et al.*, 2012). Epicardial cells contribute to heart development in two main ways. First, factors derived from the epicardium promote myocardial growth and the development of coronary vasculature (Chen *et al.*, 2002; Stuckmann *et al.*, 2003; Lavine *et al.*, 2005; Merki *et al.*, 2005; Compton *et al.*, 2007; Zamora *et al.*, 2007; Mellgren *et al.*, 2008). Second, a subset of epicardial cells can undergo an epithelial-to-mesenchymal transition (EMT) and migrate into the myocardium, where they can then differentiate into cardiac fibroblasts, vascular smooth muscle, and possibly coronary endothelial cells (Wilm *et al.*, 2005; Smith *et al.*, 2011; Katz *et al.*, 2012). Different signaling pathways influence epicardial cell migration (Lavine *et al.*, 2005; Compton *et al.*, 2007; Mellgren *et al.*, 2008; Wu *et al.*, 2010; von Gise *et al.*, 2011). In this study, we describe a defect in the timing of epicardial cell migration and nuclear morphology change during embryonic heart development in mice with germline knockout of *Lb1*. This work highlights the importance of *Lb1* in cell morphology and migratory behavior, as well as the use of the developing epicardium as a model for the study of these cell biological phenomena both *in vivo* and *in vitro*.

RESULTS AND DISCUSSION

***Lb1*-null epicardial cell explants exhibit an *in vitro* migration defect**

Previous studies found neuronal migration defects in *Lb1*-null embryos (Coffinier *et al.*, 2011; Kim *et al.*, 2011), but because migration is difficult to assay using cultured differentiating neuronal cells, we sought to examine this phenotype in a system more amenable to both *in vitro* and *in vivo* analysis. Epicardial cells are an ideal model system for this, as they can be readily explanted, and their biology is fairly well characterized *in vivo*. To examine migration, we explanted epicardial cells and performed either a wound-healing or Transwell chamber migration assay (Boyden, 1962; Liang *et al.*, 2007; Austin *et al.*, 2008). Epicardial cells were isolated from E12.5

heart ventricles as a highly enriched population of *Wt1*-expressing cells (Figure 1, A–H) and the number of explanted cells was similar among *Lb1*^{+/+}, *Lb1*^{+/-}, and *Lb1*^{-/-} genotypes (Figure 1I). In the scratch wound-healing assay, we measured the closure of the wound by live imaging at the indicated time points. As shown in Figure 1, J–O, wild-type epicardial cells closed the wound faster than *Lb1*-null epicardial cells. A quantitative assessment of three independent explants for each genotype (Figure 1P) shows that this defect becomes apparent around 8 h after wounding. To test this orthogonally, we measured the ability of epicardial cells from *Lb1*^{+/+}, *Lb1*^{+/-}, and *Lb1*^{-/-} embryos to spontaneously migrate in a Transwell chamber assay. We observed that the number of *Lb1*^{+/-} epicardial cells that migrated was similar to wild type, indicating that haploinsufficiency had little effect on migratory ability, whereas *Lb1*-null epicardial cells showed a significant reduction in the number of migrated cells (Figure 1Q). This result was consistent with our wound-healing assay, and we concluded that *Lb1* was necessary for efficient migration of epicardial cells *in vitro*.

Delayed *in vivo* epicardial cell migration in *Lb1*-null embryos

Epicardial cells encompass the heart by E11.0, undergo EMT, and migrate into the heart at ~E12.5, where they can later give rise to various cell types (Merki *et al.*, 2005; Wilm *et al.*, 2005; Smith *et al.*, 2011; Zeng *et al.*, 2011; Katz *et al.*, 2012; Rudat and Kispert, 2012). To investigate the possibility of an *in vivo* migration defect, we imaged confocal stacks from wild-type and *Lb1*-null heart sections at either E13.5 or E15.5 and quantitated the number of *Wt1*⁺ epicardial cells in the ventricular myocardium. We present the data as a percentage of the total number of *Wt1*⁺ cells observed. We excluded *Wt1*⁺ cells from the interventricular septum because of their uncertain origin (Rudat and Kispert, 2012). As shown in Figure 2, A–F, embryos lacking *Lb1* showed a consistent reduction in the number of *Wt1*⁺ cells present in the myocardium at E13.5 (white arrowheads). Approximately 30% of the total *Wt1*⁺ cell population could be found in the wild-type ventricular myocardium, whereas *Lb1*-null embryos had ~15% (Figure 2G). We did not observe any difference in the number of *Wt1*⁺ cells on the surface of the heart between the two genotypes, which was consistent with what we observed in our explants. In line with previous reports, *Wt1*⁺ cells were abundant in the heart myocardium at E15.5 (Rudat and Kispert, 2012). Of interest, the number of *Wt1*⁺ cells in the myocardium was similar (~70% of total) for both genotypes at E15.5 (Figure 3, H–M and N). These results suggest that the *Lb1* helps to ensure timely epicardial cell migration *in vivo*.

Altered nuclear morphology in *Lb1*-null epicardial cell *in vivo*

A previous study observed that mouse epicardial cells on the myocardium adopt a flattened cell and nuclear morphology *in vivo* (Komiya *et al.*, 1987). As seen in Figure 3, A–C, many *Wt1*-marked epicardial cell nuclei surrounding the ventricles and atria adopted a flattened nuclear morphology (arrowheads) in wild-type embryos at E13.5. By contrast, epicardial cells from similar areas of the *Lb1*-null E13.5 heart displayed an increased number of cells with a round, nuclear morphology (Figure 3, D–F, arrowheads). Quantitation of the nuclear width/height (Figure 3, M and N) from wild-type and *Lb1*-null *Wt1*⁺ epicardial cells that surrounded the ventricles showed that nuclear morphology was indeed different for many E13.5 epicardial cells (Figure 3O). To examine the possibility of an effect of the *Lb1*-null genotype on other nuclear envelope components in epicardial cells, we stained wild-type and *Lb1*-null E13.5 hearts for both lamin A/C and *Wt1*. As seen in Supplemental Figure 1, A–H, both wild-type and *Lb1*-null epicardial cells showed similar lamin

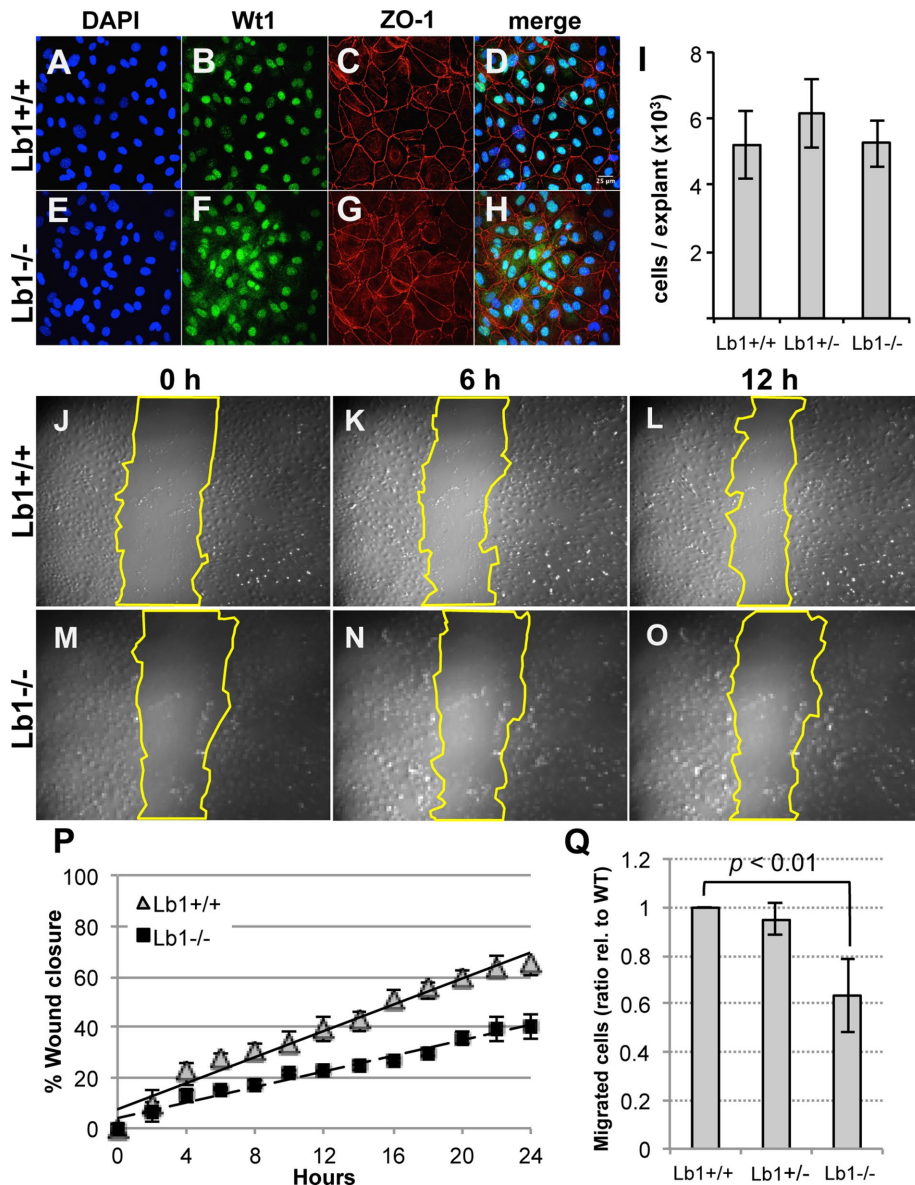


FIGURE 1: *Lb1*-null epicardial cells show a migration defect in vitro. Representative images of wild-type (A–D) and *Lb1*^{-/-} (E–H) E12.5 epicardial explants stained as indicated. Scale bar, 25 μ m. (I) Quantitation of the number of *Lb1*^{+/+}, *Lb1*^{+/-}, and *Lb1*^{-/-} epicardial cells obtained from the explant procedure (at least four explants). Error bars present SEM. (J–O) Representative images from the wound-healing assay using wild-type (J–L) and *Lb1*-null (M–O) epicardial cells. (P) The area between the wounds was measured from three independent samples at the indicated time points, and the mean was plotted (the error bars represent SD). (Q) Quantification of migration of wild-type, *Lb1*^{+/-}, and *Lb1*^{-/-} epicardial cells assessed using a Transwell chamber assay from three independent experiments. Error bars represent SD of the mean.

A/C staining. We note that populations of round Wt1⁺ cells were abundant in the caudal region of the ventricles in both wild-type and *Lb1*-null E13.5 animals (Supplemental Figure S1).

We next asked whether the difference in nuclear morphology was transient. Examining Wt1⁺ epicardial cells from wild-type and *Lb1*-null embryos at E15.5 revealed that the nuclear morphology appeared to be similar (Figure 3, G–L), and quantitative measurement of nuclear width/height revealed only a subtle difference between the two genotypes (Figure 3P). To rule out a technical artifact, we used a different fixation method (Bouin's fixative) and paraffin embedment of our samples. In agreement with our finding, we

observed that epicardial cell nuclei from *Lb1*-null embryos were rounder than wild-type counterparts at E13.5 (Supplemental Figure 1, J and K). Explanted *Lb1*-null epicardial cells showed occasional blebbing in vitro, which was apparent by 4',6-diamidino-2-phenylindole (DAPI), but with no other obvious defects (Supplemental Figure S1, L and M). These data suggest that *Lb1* loss results in a delayed morphological change in epicardial cells in vivo.

***Lb1*-null embryos show poor growth of the compact myocardium and incomplete development of the smooth muscle cell layer surrounding the coronary vessels**

The ventricular myocardium increases in thickness between E11.5 and E14, and since the epicardium contributes to embryonic myocardial growth, we examined the possibility of a defect in compact myocardium development in *Lb1*-null embryos (Chen *et al.*, 2002; Stuckmann *et al.*, 2003; Lavine *et al.*, 2005; Merki *et al.*, 2005; Mellgren *et al.*, 2008; Savolainen *et al.*, 2009). Hematoxylin and eosin staining of paraffin-embedded sections revealed that the ratio of ventricular compact myocardium (marked by white double-headed arrows) to overall heart diameter was roughly equal at E12.5 (Figure 4, A and B) but was lower in E16.5 *Lb1*-null embryos compared with wild type (Figure 4, C–E). Although we cannot rule out effects of the germline *Lb1*-null genotype on cardiomyocytes and other cells of the heart, it is possible that epicardial cell migratory defects contribute to the delayed stimulation of myocardial growth. Future work is needed to distinguish between these possibilities. As described previously, *Lb1*-null embryos were smaller and failed to develop to a weight that was comparable to that of wild type (Kim *et al.*, 2011; Supplemental Figure S2, A and B).

Epicardial cells are believed to give rise to >90% of the cardiac vascular smooth muscle cells that surround the coronary vessels (Merki *et al.*, 2005; Wilm *et al.*, 2005; Cai *et al.*, 2008). We therefore speculated that the migratory delay might lead to a deficiency in vascular smooth muscle cell development. To examine this, we stained E18.5 hearts from wild-type and *Lb1*-null embryos for markers of endothelial cells (CD31) and smooth muscle cells (smooth muscle actin) and imaged a confocal z-series for analysis. As seen in Figure 4, F–H, wild-type embryos showed continuous smooth muscle actin staining around the coronary vessel, whereas *Lb1*-null embryos often had fragmented or incomplete smooth muscle actin staining (Figure 4, I–K). Quantitation for vessels with continuous smooth muscle actin staining (defined as a continuous staining in at least two consecutive z-images; Figure 4L) showed that ~75% of wild-type coronary vessels had continuous staining, whereas only

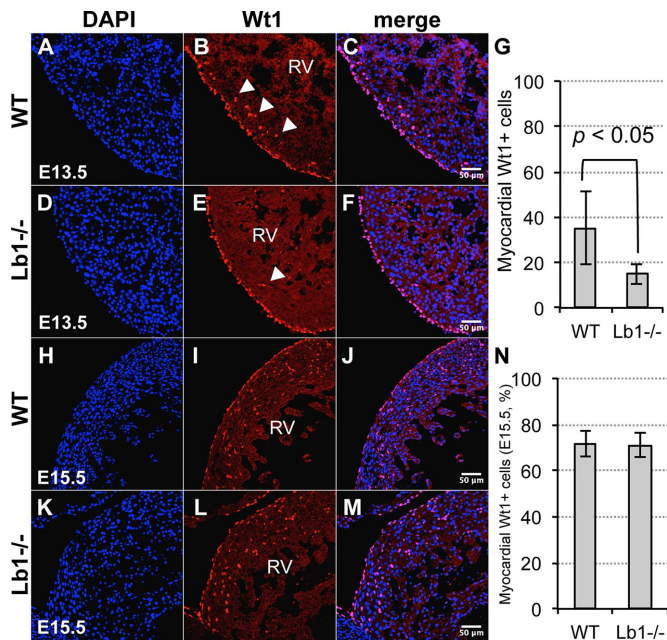


FIGURE 2: A reduced number of Wt1+ epicardial cells in the myocardium in vivo. (A–C) Wild-type E13.5, (D–F) *Lb1*^{-/-} E13.5, (H–J) wild-type E15.5, and (K–M) *Lb1*^{-/-} E15.5 sections were stained for DAPI and Wt1 as indicated. Representative images of the right ventricle (RV). Myocardial Wt1⁺ cells were quantitated from (G) E13.5 and (N) E15.5 confocal stacks and are presented as percentage of the total number of Wt1⁺ cells. Error bars represent SD. At least 300 Wt1⁺ cells were counted from three independent samples. Scale bars, 50 μ m.

~20% of the coronary vessels in *Lb1*-null embryos met this criterion. These results indicate that *Lb1*-null embryos have poor development of the compact myocardial layer and incomplete formation of vascular smooth muscle around coronary vessels. This suggests that the epicardial layer is one source of the observed defects.

Gene expression change in *Lb1*-null epicardial cells

Lb1 has been shown to influence the expression of certain genes, some of which may contribute to cell migration (Dechat *et al.*, 2010). To explore this possibility, we performed triplicate RNA-sequencing experiments on wild-type and *Lb1*-null epicardial cell explants and considered a gene to be affected by *Lb1* loss only if the change was observed in all three replicates. We found that *Lb1* loss in epicardial cells resulted in the transcriptional up- and down-regulation of 122 and 160 genes, respectively. DAVID Gene Ontology (GO) analyses showed that many up-regulated GO terms were related to immune response function (Figure 5A). Of interest, both *Lb1* reduction and increased secretion of proinflammatory cytokines and chemokines are linked to cell senescence (Coppe *et al.*, 2008; Freund *et al.*, 2012). In addition, in the *Drosophila* fat body, both age-associated lamin-B (*Drosophila* only has one B-type lamin) reduction and genetic knockdown of lamin-B in young flies increased the expression of immune-responsive genes and systemic inflammation (Chen *et al.*, 2014). Taken together, these findings suggest that lamin-B is involved in repressing immune-responsive genes during embryonic development and adult stages.

The most significant down-regulated GO terms are related to cell adhesion and the extracellular matrix function, categories relevant to cell migration (Figure 5B). Of note, we also observed the transcriptional up-regulation of extracellular protease modulators (Serp1b9b, Tfp12; Figure 5C), which have known roles in cell migration (Gessler

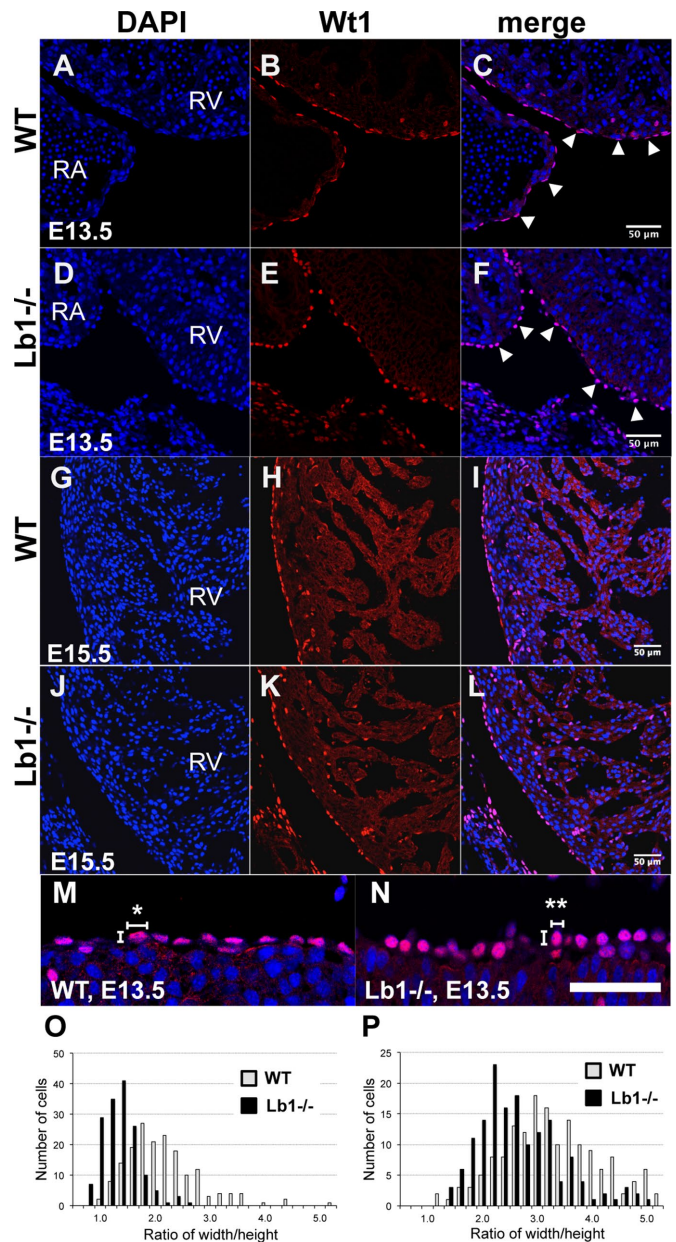


FIGURE 3: Epicardial cells from *Lb1*^{-/-} embryos show a delayed change in nuclear shape. (A–C) Wild-type embryos (E13.5) stained for DAPI (DNA) and Wt1 (epicardial cell marker) and the resulting merge image as indicated. Colocalization of DAPI and Wt1 appears magenta. (D–F) E13.5 *Lb1*^{-/-} embryos were stained as described for wild type. (G–I) Wild-type and (J–L) *Lb1*^{-/-} embryos at E15.5 were stained as described. Quantitation of epicardial cell nuclear width/height in (M) wild-type and (N) *Lb1*^{-/-} hearts. Width was measured parallel to the heart surface, and height was measured perpendicular to the heart surface. The asterisk indicates an example of the flattened morphology and the double asterisk an example of the round morphology. Distribution of nuclear width/height is shown for (O) E13.5 and (P) E15.5. Wild-type samples are gray bars, and *Lb1*^{-/-} embryos are black bars. Three independent embryos were assessed, and at least 50 epicardial cells were quantitated from each embryo. Scale bars, 50 μ m. Arrowheads point to examples of Wt1⁺ epicardial cells with different morphologies. RA, right atrium; RV, right ventricle.

et al., 2011; Lee and Yutzey, 2011). Further, some modulators of the transforming growth factor β (TGF β) pathway, which are important to epicardial cell biology and migration, were deregulated. These

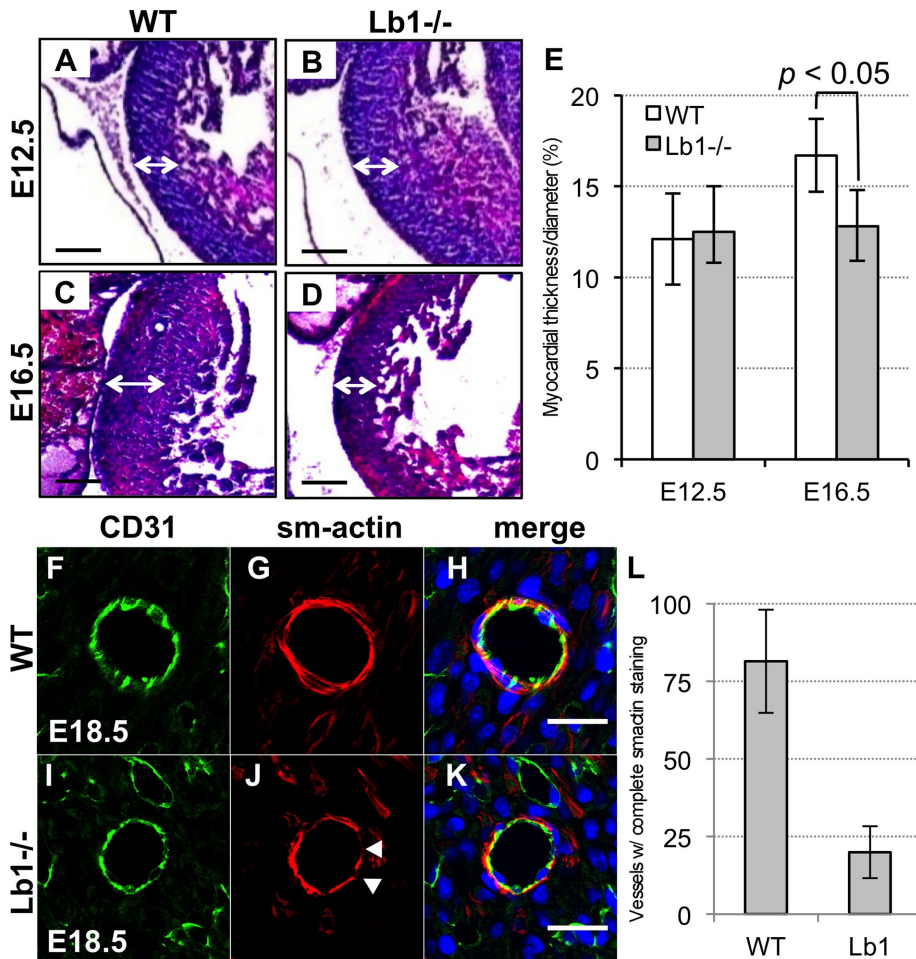


FIGURE 4: *Lb1*^{-/-} embryos show a reduced compact myocardium layer and discontinuous smooth muscle surrounding the coronary vessels. Comparison of compact myocardium thickness (white double-headed arrows) stained with hematoxylin and eosin from E12.5 (A) wild-type and (B) *Lb1*^{-/-} and E16.5 (C) wild-type and (D) *Lb1*^{-/-} embryos. Scale bar, 100 μ m. (E) Quantification of compact myocardium thickness normalized to heart diameter. Quantification was performed on at least six different embryos. Error bars indicate SD of the mean. (F–H) Wild-type E18.5 embryos were stained for CD31 (endothelial cell) and smooth muscle actin (“sm actin”; smooth muscle cell) and merged as indicated. (I–K) *Lb1*^{-/-} E18.5 embryos were stained as described for wild type. Arrowheads point to examples of fragmented staining. Scale bar, 25 μ m. (L) Quantitation of the mean percentage of coronary vessels with continuous smooth muscle staining from at least three wild-type and *Lb1*^{-/-} E18.5 samples. Error bars represent SD of the mean. Smooth muscle actin staining was classified as either 1) continuous staining around the vessel in at least two consecutive sections or 2) discontinuous staining in at least two consecutive sections.

included *Noggin* (*Nog*), an inhibitor of TGF β signaling; *Adamtsl2*, a regulator of TGF β availability; and *Periostin* (*Postn*), a downstream target of TGF β signaling that is linked to the migration of epicardial cells (Figure 5C; Compton *et al.*, 2007; Le Goff *et al.*, 2008; Sridurongrit *et al.*, 2008; Snider *et al.*, 2009; Ishii *et al.*, 2010; Zhou *et al.*, 2010). As validation, we performed quantitative reverse transcriptase PCR (qRT-PCR) analyses of select genes involved in TGF β signaling (Figure 5D). Thus *Lb1* loss appears to affect the transcription of a set of genes with importance to cell migratory behavior and likely contributes to the observed migratory delay.

Conclusion

In this study, we identified a delay in epicardial cell migration in *Lb1*-null embryos that was recapitulated *in vitro* using explanted epicardial cells. Further, *Lb1*-null embryos showed a delayed change

in epicardial cell nuclear morphology, which is not well understood in this context and was not apparent *in vitro*. Instead, explanted epicardial cells lacking *Lb1* were largely normal except for the presence of a minor population of cells with nuclear membrane blebbing, a hallmark of some lamin mutant cells cultured *in vitro*. Considering the cellular roles of *Lb1*, we speculate that a timely nuclear morphology change in the epicardium, which may contribute to proper expression of certain genes, including those involved in cell adhesion, might be important for cell migration behavior. Alternatively, *Lb1* may regulate these genes by influencing the three-dimensional chromatin organization. Although we did not observe an obvious detachment of the epicardium from the hearts of *Lb1*^{-/-} embryos, we cannot rule out the possibility of other changes in the extracellular matrix, or the remodeling thereof, that are beyond the limits of detection. Additional, nontranscriptional roles for *Lb1* should be considered, as they are known to be important for cell migration. For instance, *Lb1* levels modulate the rebound elasticity of the nucleus during cell migration and also helps to connect the nucleus to the cytoskeleton via the Linker of Nucleoskeleton to Cytoskeleton (LINC) complex (Ji *et al.*, 2007; Shin *et al.*, 2013; Harada *et al.*, 2014; Chang *et al.*, 2015b). Overall our work highlights the importance of *Lb1* to cell migratory behavior and also demonstrates the use of the epicardial cell system to study changes in cell morphology and migration both *in vivo* and *in vitro*. This system should be valuable for the further elucidation of the relationship between these cell biological phenomena.

MATERIALS AND METHODS

Animals

All animal work was done in accordance with the guidelines set forth by the Carnegie Institution Animal Care and Use Committee. *Lb1*-knockout mouse model was previously described (Kim *et al.*, 2011). Mice were

housed under a 12-h/12-h light/dark cycle and fed *ad libitum*. Dams were killed by either cervical dislocation or CO₂ asphyxiation.

Histology

Embryos were isolated at the indicated times and fixed in 4% Formalin for 24 h at 4°C before embedding in either paraffin or O.C.T. (Tissue Tek, Torrance, CA). Before O.C.T. embedding, embryos were saturated in 30% sucrose for 24 h at 4°C. Paraffin-embedded sections were prepared and dehydrated before hematoxylin and eosin staining. O.C.T.-embedded sections were used for immunofluorescence (described later).

Immunofluorescence

O.C.T.-embedded sections were cut on a Leica CM3050S cryostat to a 10–12 μ m thickness and attached to Superfrost microscope

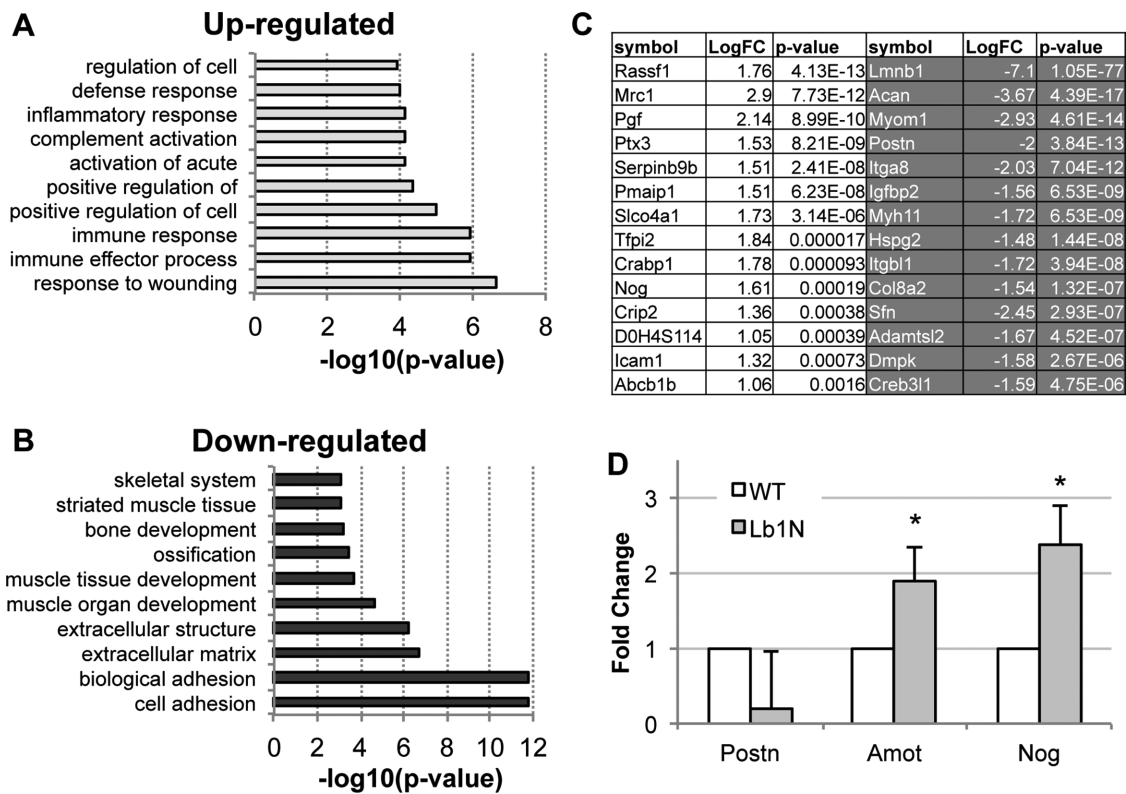


FIGURE 5: *Lb1* loss affects gene expression in epicardial cells. DAVID GO term analysis for (A) up-regulated and (B) down-regulated genes from *Lb1*-null epicardial explants compared with that of the wild type. (C) Examples of up-regulated (light background) and down-regulated (dark background) genes. (D) qRT-PCR validation of select deregulated genes from three independent wild-type and *Lb1*^{-/-} epicardial cell explants. Error bars indicate SD; **p* < 0.05.

slides (12-550-15; Fisher, Rockford, MA). Heat-induced antigen retrieval was done with sodium citrate, pH 6.0, supplemented with Tween-20. Retrieved sections were permeabilized with phosphate-buffered saline (PBS) containing 0.25% Triton X-100 and blocked with PBS containing 10% bovine serum albumin, 10% normal goat serum, and M.O.M blocking agent (MKB-2213; Vector Labs, Burlingame, CA). Primary and secondary antibodies were diluted in the same blocking buffer. Primary antibodies were incubated at 4°C overnight, and secondary antibodies were incubated for 2 h at room temperature. All washing steps were performed with PBS, and DAPI at 1 µg/ml was used to stain DNA. Epicardial explants (see later description) were fixed with 4% Formalin and processed as described. Antibodies used in this study are indicated next.

Antibodies

Antibodies used and their respective dilutions are as follows. Rabbit anti-Wt1 (sc-192, 1:20; Santa Cruz Biotechnology, Santa Cruz, CA), rabbit anti-CD31 (ab28364, 1:50; Abcam, Cambridge, MA), mouse anti-smooth muscle actin, α -Cy3 (C6198, 1:100; Sigma-Aldrich, St. Louis, MO), rat anti-ZO-1 (R26.4C-c, 1:50; Developmental Studies Hybridoma Bank, Iowa City, IA), and mouse anti-lamin A/C (39287, 1:100; Active Motif, Carlsbad, CA). Alexa Fluor-conjugated secondary antibodies (1:1000) were either goat anti-rabbit or rat and are available from Invitrogen/Molecular Probes.

Imaging

Hematoxylin and eosin-stained sections were imaged with a Leica M125 microscope using Leica LAS EZ software. Immunofluorescence imaging was done using a Leica SP5 laser-scanning confocal microscope using Leica LAS AF software. Bright-field imaging of

epicardial explant for cell number quantitation was done using a Nikon Eclipse TE200 inverted microscope. Live imaging of epicardial explants used in the wound-healing assay was done using a Nikon Eclipse TE2000U equipped with a Pathology Devices LiveCell controller for temperature, humidity, and CO₂ regulation. MetaMorph was used for the wide-field microscopes. The Multidimensional Acquisition plug-in for MetaMorph was used for live imaging. Images were analyzed with either MetaMorph or the FIJI package of ImageJ.

Epicardial explants

Epicardial explant was done in a manner similar to that previously described but with modifications (Austin et al., 2008). Hearts from E12.5 embryos were isolated, and atria were removed with forceps (11251-20; Fine Science Tools). The remaining ventricles were placed in a gelatinized well of a 24-well plate containing 200 µl of DMEM supplemented with 10% fetal bovine serum, glutaMAX, and penicillin/streptomycin ("explant media"). The orientation of the heart was such that dorsal portion was on the surface of the well. Explant culture was done for 48 h at 37°C with 5% oxygen. After this initial culture, the heart was removed, and the remaining explant was washed with PBS. Explants were then grown for an additional 72 h in explant media before any other subsequent procedures. For immunofluorescence of epicardial explants, the heart was placed on a gelatinized circular coverglass (12-545-80; Fisher) in a 24-well plate, and the foregoing procedures were followed.

Wound-healing assay

The wound-healing assay was performed as previously described but with modification (Liang et al., 2007). Epicardial explants were

scratched with a sterile 10- μ l pipet tip, followed by washing with PBS. Explant medium was added, and the wound was imaged as described in the *Imaging* section at the indicated time points. The amount of wound closure was measured by quantitating the intervening area with ImageJ 1.46r software. Graphical representation is the mean \pm SD from three independent experiments.

Transwell chamber assay

Multiple epicardial explants of the same genotype were pooled and counted with a hemocytometer. Approximately 20,000 epicardial cells of the indicated genotype were seeded in a 100- μ l volume of explant medium in the upper chamber of the Transwell apparatus (351163; BD, San Jose, CA). The lower chamber contained a 150- μ l volume of explant medium. The culture was then incubated for 24 h at 37°C with 5% oxygen. Afterward, the insert was removed, and the original seeding was detached with a cotton swab. The insert was then fixed in 4% Formalin, permeabilized, and stained with DAPI, and the cells that had migrated to the opposite side of the insert were imaged by confocal microscopy. Quantitation is presented as a ratio relative to wild type \pm SD.

RNA-sequencing

Total epicardial cell RNA was isolated using the Arcturus PicoPure RNA (Invitrogen) isolation kit according to the manufacturer's instruction. Libraries were constructed using the Illumina TrueSeq RNA library kit, version 2.0, and sequenced using an Illumina HiSeq 2000. Reads were mapped using Bowtie 2.0, and expression was analyzed using the Cufflinks package. Genes with RPKM (reads per kilobase of transcript per million mapped reads) < 2 were discarded. Further analysis was done in R using the EdgeR library. Charts were produced using Excel (Microsoft). GO term analysis was performed using the DAVID web interface (National Institutes of Health; <https://david.ncifcrf.gov/>). RNA-sequencing data are available (GEO accession GSE87344; www.ncbi.nlm.nih.gov/geo/). Validation of RNA-sequencing data was done by qRT-PCR using iQ Sybr Green Mastermix (Bio-Rad) on a Bio-Rad CFX96 Real Time System.

ACKNOWLEDGMENTS

We thank Ona Martin for technical assistance, Mahmud Siddiqi for assistance with microscopy, and other lab members for suggestions and discussions. We are grateful to Helan Xiao for great assistance during this study. This study was supported by a Senior Scholar Award to Y.Z. from the Ellison Medical Foundation and National Institutes of Health Grants GM056312 and GM106023 (Y.Z.).

REFERENCES

Austin AF, Compton LA, Love JD, Brown CB, Barnett JV (2008). Primary and immortalized mouse epicardial cells undergo differentiation in response to TGF β . *Dev Dyn* 237, 366–376.

Bonne G, Di Barletta MR, Varnous S, Becane HM, Hammouda EH, Merlini L, Muntoni F, Greenberg CR, Gary F, Urtizberea JA, et al. (1999). Mutations in the gene encoding lamin A/C cause autosomal dominant Emery-Dreifuss muscular dystrophy. *Nat Genet* 21, 285–288.

Boyden S (1962). The chemotactic effect of mixtures of antibody and antigen on polymorphonuclear leucocytes. *J Exp Med* 115, 453–466.

Burke B, Stewart CL (2013). The nuclear lamins: flexibility in function. *Nat Rev Mol Cell Biol* 14, 13–24.

Cai CL, Martin JC, Sun Y, Cui L, Wang L, Ouyang K, Yang L, Bu L, Liang X, Zhang X, et al. (2008). A myocardial lineage derives from Tbx18 epicardial cells. *Nature* 454, 104–108.

Chang W, Antoku S, Ostlund C, Worman HJ, Gundersen GG (2015a). Linker of nucleoskeleton and cytoskeleton (LINC) complex-mediated actin-dependent nuclear positioning orients centrosomes in migrating myoblasts. *Nucleus* 6, 77–88.

Chang W, Worman HJ, Gundersen GG (2015b). Accessorizing and anchoring the LINC complex for multifunctionality. *J Cell Biol* 208, 11–22.

Chen H, Chen X, Zheng Y (2013). The nuclear lamina regulates germline stem cell niche organization via modulation of EGFR signaling. *Cell Stem Cell* 13, 73–86.

Chen H, Zheng X, Zheng Y (2014). Age-associated loss of lamin-B leads to systemic inflammation and gut hyperplasia. *Cell* 159, 829–843.

Chen H, Zheng X, Zheng Y (2015). Lamin-B in systemic inflammation, tissue homeostasis, aging. *Nucleus* 6, 183–186.

Chen T, Chang TC, Kang JO, Choudhary B, Makita T, Tran CM, Burch JB, Eid H, Sucov HM (2002). Epicardial induction of fetal cardiomyocyte proliferation via a retinoic acid-inducible trophic factor. *Dev Biol* 250, 198–207.

Coffinier C, Jung HJ, Nobumori C, Chang S, Tu Y, Barnes RH 2nd, Yoshinaga Y, de Jong PJ, Vergnes L, Reue K, Fong LG, Young SG (2011). Deficiencies in lamin B1 and lamin B2 cause neurodevelopmental defects and distinct nuclear shape abnormalities in neurons. *Mol Biol Cell* 22, 4683–4693.

Compton LA, Potash DA, Brown CB, Barnett JV (2007). Coronary vessel development is dependent on the type III transforming growth factor beta receptor. *Circ Res* 101, 784–791.

Coppe JP, Patil CK, Rodier F, Sun Y, Munoz DP, Goldstein J, Nelson PS, Desprez PY, Campisi J (2008). Senescence-associated secretory phenotypes reveal cell-nonautonomous functions of oncogenic RAS and the p53 tumor suppressor. *PLoS Biol* 6, 2853–2868.

Dahl KN, Ribeiro AJ, Lammerding J (2008). Nuclear shape, mechanics, and mechanotransduction. *Circ Res* 102, 1307–1318.

Davidson PM, Denais C, Bakshi MC, Lammerding J (2014). Nuclear deformability constitutes a rate-limiting step during cell migration in 3-D environments. *Cell Mol Bioeng* 7, 293–306.

Dechat T, Adam SA, Taimen P, Shimi T, Goldman RD (2010). Nuclear lamins. *Cold Spring Harb Perspect Biol* 2, a000547.

De Sandre-Giovannoli A, Bernard R, Cau P, Navarro C, Amiel J, Boccaccio I, Lyonnet S, Stewart CL, Munnich A, Le Merrer M, Levy N (2003). Lamin A truncation in Hutchinson-Gilford progeria. *Science* 300, 2055.

Eriksson M, Brown WT, Gordon LB, Glynn MW, Singer J, Scott L, Erdos MR, Robbins CM, Moses TY, Berglund P, et al. (2003). Recurrent de novo point mutations in lamin A cause Hutchinson-Gilford progeria syndrome. *Nature* 423, 293–298.

Fatkin D, MacRae C, Sasaki T, Wolff MR, Porcu M, Frenneaux M, Atherton J, Vidaillet HJ Jr, Spudich S, De Girolami U, Seidman JG, et al. (1999). Missense mutations in the rod domain of the lamin A/C gene as causes of dilated cardiomyopathy and conduction-system disease. *N Engl J Med* 341, 1715–1724.

Freund A, Laberge RM, Demaria M, Campisi J (2012). Lamin B1 loss is a senescence-associated biomarker. *Mol Biol Cell* 23, 2066–2075.

Gessler F, Voss V, Seifert V, Gerlach R, Kogel D (2011). Knockdown of TFPI-2 promotes migration and invasion of glioma cells. *Neurosci Lett* 497, 49–54.

Goldman RD, Shumaker DK, Erdos MR, Eriksson M, Goldman AE, Gordon LB, Gruenbaum Y, Khuon S, Mendez M, Varga R, Collins FS (2004). Accumulation of mutant lamin A causes progressive changes in nuclear architecture in Hutchinson-Gilford progeria syndrome. *Proc Natl Acad Sci USA* 101, 8963–8968.

Gruenbaum Y, Foisner R (2015). Lamins: nuclear intermediate filament proteins with fundamental functions in nuclear mechanics and genome regulation. *Annu Rev Biochem* 84, 131–164.

Guelen L, Pagie L, Brasset E, Meuleman W, Faza MB, Talhout W, Eussen BH, de Klein A, Wessels L, de Laat W, van Steensel B (2008). Domain organization of human chromosomes revealed by mapping of nuclear lamina interactions. *Nature* 453, 948–951.

Guillemin K, Williams T, Krasnow MA (2001). A nuclear lamin is required for cytoplasmic organization and egg polarity in *Drosophila*. *Nat Cell Biol* 3, 848–851.

Guo Y, Kim Y, Shimi T, Goldman RD, Zheng Y (2014). Concentration-dependent lamin assembly and its roles in the localization of other nuclear proteins. *Mol Biol Cell* 25, 1287–1297.

Guo Y, Zheng Y (2015). Lamins position the nuclear pores and centrosomes by modulating dynein. *Mol Biol Cell* 26, 3379–3389.

Harada T, Swift J, Irianto J, Shin JW, Spinler KR, Athirasala A, Diegmiller R, Dingal PC, Ivanovska IL, Discher DE (2014). Nuclear lamin stiffness is a barrier to 3D migration, but softness can limit survival. *J Cell Biol* 204, 669–682.

Hernandez L, Roux KJ, Wong ES, Mounkes LC, Mutalif R, Navasankari R, Rai B, Cool S, Jeong JW, Wang H, et al. (2010). Functional coupling

- between the extracellular matrix and nuclear lamina by Wnt signaling in progeria. *Dev Cell* 19, 413–425.
- Imai S, Nishibayashi S, Takao K, Tomifuji M, Fujino T, Hasegawa M, Takano T (1997). Dissociation of Oct-1 from the nuclear peripheral structure induces the cellular aging-associated collagenase gene expression. *Mol Biol Cell* 8, 2407–2419.
- Ishii Y, Garriock RJ, Navetta AM, Coughlin LE, Mikawa T (2010). BMP signals promote proepicardial protrusion necessary for recruitment of coronary vessel and epicardial progenitors to the heart. *Dev Cell* 19, 307–316.
- Ji JY, Lee RT, Vergnes L, Fong LG, Stewart CL, Reue K, Young SG, Zhang Q, Shanahan CM, Lammerding J (2007). Cell nuclei spin in the absence of lamin b1. *J Biol Chem* 282, 20015–20026.
- Jung HJ, Nobumori C, Goulbourne CN, Tu Y, Lee JM, Tatar A, Wu D, Yoshinaga Y, de Jong PJ, Coffinier C, et al. (2013). Farnesylation of lamin B1 is important for retention of nuclear chromatin during neuronal migration. *Proc Natl Acad Sci USA* 110, E1923–E1932.
- Katz TC, Singh MK, Degenhardt K, Rivera-Feliciano J, Johnson RL, Epstein JA, Tabin CJ (2012). Distinct compartments of the proepicardial organ give rise to coronary vascular endothelial cells. *Dev Cell* 22, 639–650.
- Kim DH, Cho S, Wirtz D (2014). Tight coupling between nucleus and cell migration through the perinuclear actin cap. *J Cell Sci* 127, 2528–2541.
- Kim Y, Sharov AA, McDole K, Cheng M, Hao H, Fan CM, Gaiano N, Ko MS, Zheng Y (2011). Mouse B-type lamins are required for proper organogenesis but not by embryonic stem cells. *Science* 334, 1706–1710.
- Kim Y, Zheng X, Zheng Y (2013). Proliferation and differentiation of mouse embryonic stem cells lacking all lamins. *Cell Res* 23, 1420–1423.
- Komiyama M, Ito K, Shimada Y (1987). Origin and development of the epicardium in the mouse embryo. *Anat Embryol* 176, 183–189.
- Lammerding J, Fong LG, Ji JY, Reue K, Stewart CL, Young SG, Lee RT (2006). Lamins A and C but not lamin B1 regulate nuclear mechanics. *J Biol Chem* 281, 25768–25780.
- Lammermann T, Bader BL, Monkley SJ, Worbs T, Wedlich-Soldner R, Hirscher K, Keller M, Forster R, Critchley DR, Fassler R, Sixt M (2008). Rapid leukocyte migration by integrin-independent flowing and squeezing. *Nature* 453, 51–55.
- Lautscham LA, Kammerer C, Lange JR, Kolb T, Mark C, Schilling A, Strissel PL, Strick R, Gluth C, Rowat AC, et al. (2015). Migration in confined 3D environments is determined by a combination of adhesiveness, nuclear volume, contractility, and cell stiffness. *Biophys J* 109, 900–913.
- Lavine KJ, Yu K, White AC, Zhang X, Smith C, Partanen J, Ornitz DM (2005). Endocardial and epicardial derived FGF signals regulate myocardial proliferation and differentiation in vivo. *Dev Cell* 8, 85–95.
- Lee JS, Hale CM, Panorchan P, Khataou SB, George JP, Tseng Y, Stewart CL, Hodzic D, Wirtz D (2007). Nuclear lamin A/C deficiency induces defects in cell mechanics, polarization, and migration. *Biophys J* 93, 2542–2552.
- Lee MP, Yutzev KE (2011). Twist1 directly regulates genes that promote cell proliferation and migration in developing heart valves. *PLoS One* 6, e29758.
- Le Goff C, Morice-Picard F, Dagonneau N, Wang LW, Perrot C, Crow YJ, Bauer F, Flori E, Prost-Squarcioni C, Krakow D, et al. (2008). ADAMTSL2 mutations in geleophysic dysplasia demonstrate a role for ADAMTS-like proteases in TGF-beta bioavailability regulation. *Nat Genet* 40, 1119–1123.
- Liang CC, Park AY, Guan JL (2007). In vitro scratch assay: a convenient and inexpensive method for analysis of cell migration in vitro. *Nat Protoc* 2, 329–333.
- Liu J, Rolf Ben-Shahar T, Riemer D, Treinin M, Spann P, Weber K, Fire A, Gruenbaum Y (2000). Essential roles for Caenorhabditis elegans lamin gene in nuclear organization, cell cycle progression, and spatial organization of nuclear pore complexes. *Mol Biol Cell* 11, 3937–3947.
- Mellgren AM, Smith CL, Olsen GS, Eskioçak B, Zhou B, Kazi MN, Ruiz FR, Pu WT, Tallquist MD (2008). Platelet-derived growth factor receptor beta signaling is required for efficient epicardial cell migration and development of two distinct coronary vascular smooth muscle cell populations. *Circ Res* 103, 1393–1401.
- Merki E, Zamora M, Raya A, Kawakami Y, Wang J, Zhang X, Burch J, Kubalak SW, Kaliman P, Izpisua Belmonte JC, et al. (2005). Epicardial retinoid X receptor alpha is required for myocardial growth and coronary artery formation. *Proc Natl Acad Sci USA* 102, 18455–18460.
- Moore AW, Schedl A, McInnes L, Doyle M, Hecksher-Sorensen J, Hastie ND (1998). YAC transgenic analysis reveals Wilms' tumour 1 gene activity in the proliferating coelomic epithelium, developing diaphragm and limb. *Mech Dev* 79, 169–184.
- Muchir A, Pavlidis P, Decostre V, Herron AJ, Arimura T, Bonne G, Worman HJ (2007). Activation of MAPK pathways links LMNA mutations to cardiomyopathy in Emery-Dreifuss muscular dystrophy. *J Clin Invest* 117, 1282–1293.
- Olivey HE, Svensson EC (2010). Epicardial-myocardial signaling directing coronary vasculogenesis. *Circ Res* 106, 818–832.
- Pacheco LM, Gomez LA, Dias J, Ziebarth NM, Howard GA, Schiller PC (2014). Progerin expression disrupts critical adult stem cell functions involved in tissue repair. *Aging* 6, 1049–1063.
- Ribeiro AJ, Khanna P, Sukumar A, Dong C, Dahl KN (2014). Nuclear stiffening inhibits migration of invasive melanoma cells. *Cell Mol Bioeng* 7, 544–551.
- Rudat C, Kispert A (2012). Wt1 and epicardial fate mapping. *Circ Res* 111, 165–169.
- Savolainen SM, Foley JF, Elmore SA (2009). Histology atlas of the developing mouse heart with emphasis on E11.5 to E18.5. *Toxicol Pathol* 37, 395–414.
- Scaffidi P, Misteli T (2008). Lamin A-dependent misregulation of adult stem cells associated with accelerated ageing. *Nat Cell Biol* 10, 452–459.
- Shimi T, Butin-Israeli V, Adam SA, Hamanaka RB, Goldman AE, Lucas CA, Shumaker DK, Kosak ST, Chandel NS, Goldman RD (2011). The role of nuclear lamin B1 in cell proliferation and senescence. *Genes Dev* 25, 2579–2593.
- Shin JW, Spinler KR, Swift J, Chasis JA, Mohandas N, Discher DE (2013). Lamins regulate cell trafficking and lineage maturation of adult human hematopoietic cells. *Proc Natl Acad Sci USA* 110, 18892–18897.
- Smith CL, Baek ST, Sung CY, Tallquist MD (2011). Epicardial-derived cell epithelial-to-mesenchymal transition and fate specification require PDGF receptor signaling. *Circ Res* 108, e15–e26.
- Snider P, Standley KN, Wang J, Azhar M, Doetschman T, Conway SJ (2009). Origin of cardiac fibroblasts and the role of periostin. *Circ Res* 105, 934–947.
- Sridurongrit S, Larsson J, Schwartz R, Ruiz-Lozano P, Kaartinen V (2008). Signaling via the Tgf-beta type I receptor Alk5 in heart development. *Dev Biol* 322, 208–218.
- Stuckmann I, Evans S, Lassar AB (2003). Erythropoietin and retinoic acid, secreted from the epicardium, are required for cardiac myocyte proliferation. *Dev Biol* 255, 334–349.
- Sullivan T, Escalante-Alcalde D, Bhatt H, Anver M, Bhat N, Nagashima K, Stewart CL, Burke B (1999). Loss of A-type lamin expression compromises nuclear envelope integrity leading to muscular dystrophy. *J Cell Biol* 147, 913–920.
- Tran JR, Chen H, Zheng X, Zheng Y (2016). Lamin in inflammation and aging. *Curr Opin Cell Biol* 40, 124–130.
- Tsai MY, Wang S, Heidinger JM, Shumaker DK, Adam SA, Goldman RD, Zheng Y (2006). A mitotic lamin B matrix induced by RanGTP required for spindle assembly. *Science* 311, 1887–1893.
- Vergnes L, Peterfy M, Bergo MO, Young SG, Reue K (2004). Lamin B1 is required for mouse development and nuclear integrity. *Proc Natl Acad Sci USA* 101, 10428–10433.
- von Gise A, Pu WT (2012). Endocardial and epicardial epithelial to mesenchymal transitions in heart development and disease. *Circ Res* 110, 1628–1645.
- von Gise A, Zhou B, Honor LB, Ma Q, Petryk A, Pu WT (2011). WT1 regulates epicardial epithelial to mesenchymal transition through beta-catenin and retinoic acid signaling pathways. *Dev Biol* 356, 421–431.
- Wilm B, Ipenberg A, Hastie ND, Burch JB, Bader DM (2005). The serosal mesothelium is a major source of smooth muscle cells of the gut vasculature. *Development* 132, 5317–5328.
- Wolf K, Te Lindert M, Krause M, Alexander S, Te Riet J, Willis AL, Hoffman RM, Figdor CG, Weiss SJ, Friedl P (2013). Physical limits of cell migration: control by ECM space and nuclear deformation and tuning by proteolysis and traction force. *J Cell Biol* 201, 1069–1084.
- Wu M, Smith CL, Hall JA, Lee I, Luby-Phelps K, Tallquist MD (2010). Epicardial spindle orientation controls cell entry into the myocardium. *Dev Cell* 19, 114–125.
- Zamora M, Manner J, Ruiz-Lozano P (2007). Epicardium-derived progenitor cells require beta-catenin for coronary artery formation. *Proc Natl Acad Sci USA* 104, 18109–18114.
- Zeng B, Ren XF, Cao F, Zhou XY, Zhang J (2011). Developmental patterns and characteristics of epicardial cell markers Tbx18 and Wt1 in murine embryonic heart. *J Biomed Sci* 18, 67.
- Zheng X, Kim Y, Zheng Y (2015). Identification of lamin B-regulated chromatin regions based on chromatin landscapes. *Mol Biol Cell* 26, 2685–2697.
- Zhou B, von Gise A, Ma Q, Hu YW, Pu WT (2010). Genetic fate mapping demonstrates contribution of epicardium-derived cells to the annulus fibrosus of the mammalian heart. *Dev Biol* 338, 251–261.